ESTIMATION OF MANGROVE CARBON STOCK WITH HYBRID METHOD USING IMAGE SENTINEL-2

*Firman Farid Muhsoni[12], Abu Bakar Sambah[3], Muhammad Mahmudi[3], Dewa Gede Raka Wiadnya[3]

[1]Post-Graduate Program, Faculty of Fisheries and Marine Science, University of Brawijaya, Indonesia
[2]Marine Science Department, University of Trunojoyo Madura, Indonesia
[3]Faculty of Fisheries and Marine Science, University of Brawijaya, Indonesia

*Corresponding Author, Received: 18 May. 2018, Revised: 8 June 2018, Accepted: 18 June 2018

ABSTRACT: Field survey data combined with remote sensing data were an ideal and practical method for estimating carbon stocks. The objective of this research was to get an estimation model of mangrove carbon stock with good accuracy. Modeling used hybrid methods, by combining satellite image analysis and field data. The result of this research was to get the mangrove carbon estimation model. Model 1 merging between NNIP vegetation index equation using regression of power/geometry and six variables multiple regression (NDRE or WVVI vegetation index, sediment depth, soil density,% C soil depth 0-15 cm, 15-50 cm and >50 cm). RMSE test resulted 0.4778 t 100 m^{-2} and % RMSE 16.12%. Model 2 NNIP vegetation index and three variable regression (VIRRE vegetation index, sediment depth, soil density). RMSE test resulted 0.5639 t 100 m^{-2} and % RMSE 19.03%. Model 3 uses NNIP vegetation index and two variable regression (NDRE vegetation index and sediment depth). RMSE test resulted 0.7295 t 100 m^{-2} and RMSE % 24.63%. Model 4 incorporation of NNIP vegetation index and multiple regression of 3 variables (VIRRE vegetation index, average sediment depth value 100.63 cm, soil density value 1.02 g cm^{-3}). RMSE test resulted 1.0043 t 100 m^{-2} and % RMSE 33.89%.

Keywords: Mangrove biomass, Carbon stock, Sentinel-2 Imagery, Hybrid

1. INTRODUCTION

Mangroves could absorb carbon better than terrestrial ecosystems because of its ability to bury carbon in sediments [1]; Estimation of mangrove biomass by field survey combined with remote sensing data was an ideal and practical method [2]. The assessment of carbon stocks with remote sensing was expected to reduce destructive ways or mangrove destruction. The estimated share of mangrove carbon with remote sensing imagery has been done using various images, such Quickbird [3], ALOS, Landsat [4], and, RADARSAT [5]. Different image resolutions resulted in different model accuracy. Different types of mangroves showed significant differences in the spectral reflection of the electromagnetic spectrum. High spatial resolution images could map full carbon stocks at the mangrove species level [6].

The use of remote satellite sensing to measure the spread of biomass and mangrove carbon provided accurate, efficient, and repeatable information. Some vegetation indices such Vegetation indexes such as DVI (Difference Vegetation Index), EVI (Enhanced Vegetation Index), and MRE-SR (Modified Red Edge-Simple Ratio) with field data to estimate carbon stock [6]. The objective of the study was to obtain a mangrove carbon stock model and its accuracy using Sentinel-2 satellite images.

This survey is a continuation of a study conducted by Muhsoni et al. (2018). This study focuses on obtaining estimation models of mangrove carbon stock by a hybrid method using the Sentinel-2 image. This study can contribute to the easier estimation of mangrove carbon stock in a region more quickly and efficiently with better accuracy.

2. MATERIALS AND METHODS

2.1. Satellite Remote Sensing Data

Mangrove mapping can use Sentinel-2 satellite images (Copernicus Sentinel data (2017)). The Sentinel-2 satellite had 13 spectral bands from near-infrared to shortwave infrared. Spatial resolution varied from 10m - 60m depending on spectral band [7]. Sentinel 2 image used in this research was December 6, 2016. The channels used in this study were band 2, 3, 4, 5, 6, 8, 8a.

2.2. Pre Processing

Sentinel-2 imagery performed radiometric correction at an early stage. The radiometric correction uses the at-sensor reflectance method by changing the pixel value to the at-sensor radiance. Then converted to at-sensor reflectance [8], [9]. Mangrove area obtained by hybrid method NDVI

using threshold value from NDVI. The automatic thresholding method used was Otsu Threshold [10].

2.3. Mangrove Carbon Stock Model with Hybrid Method.

Model estimates of mangrove carbon by separating carbon and soil carbon biomass. Carbon biomass modeling (stems, roots, bottom plants) with vegetation index using nonlinear regression approach. Soil carbon estimate uses the hybrid method. Then sought the model with the best accuracy (least RMSE test).

Utilization of vegetation index in remote sensing for mapping related to vegetation [11]. Index of vegetation used 24 indexes (BR, GNDVI, GR, SAVI, MSAVI, NDRE, NDVI, NDVI2, NDWI, NNIP, PSRI, RR, RVI, VIRE, SVI, VIRE, VIRRE, MTV1, MTVI2, RDVI, VARI, VI green, MSR, and TVI). The best equation has the highest coefficient of determination (R^2) and the lowest RMSE [9], [6], [13], [14]. The regression equation used was [12]:

- Exponential : $Y = a * e^{bX}$ (1)

- Logarithmik : $Y = a + b * \ln(x)$ (2)

- Polynomial : $Y = a + bX + cX^2$ (3)

- Power/geometrik : $Y = a * X^b$ (4)

The final model with the hybrid method, by combining two approaches that use image and field measurement data [13]. This modeling performed several simulations:

- Model 1 with inputs of vegetation index values, sediment depth, soil density and % soil carbon.
- Model 2 with inputs of vegetation index values, sediment depth, and density.
- Model 3 with inputs of vegetation index values and into the soil.
- Model 4 with input only vegetation index.

2.4. Test Accuracy with RMSE.

Accuracy tests used correlation coefficient (r) and Root Mean Square Error (RMSE) [14], [15], [16], [17], [5]. Equation :

$$RMSE = \sqrt{\frac{i}{n}\sum_{i=1}^{n}(x_i - y_i)^2} \quad (5)$$

$$RMSE \% = 100 \times \frac{RMSE}{\bar{Y}} \quad (6)$$

Where: x_i =Value The carbon stock of the measurement, y_i=the predicted value of the carbon

stock, $\bar{Y}$ =the mean carbon measured [18], [19], [20], [21], [22], [23], [24], [25].

2.5. Study Area

Research location was in Pesisir Selatan district of Pamekasan, East Java, Indonesia. The number of measuring stations were 11, and each station had ten plots (Fig 1). The total plot number as the sample location sample location were 110 plots.
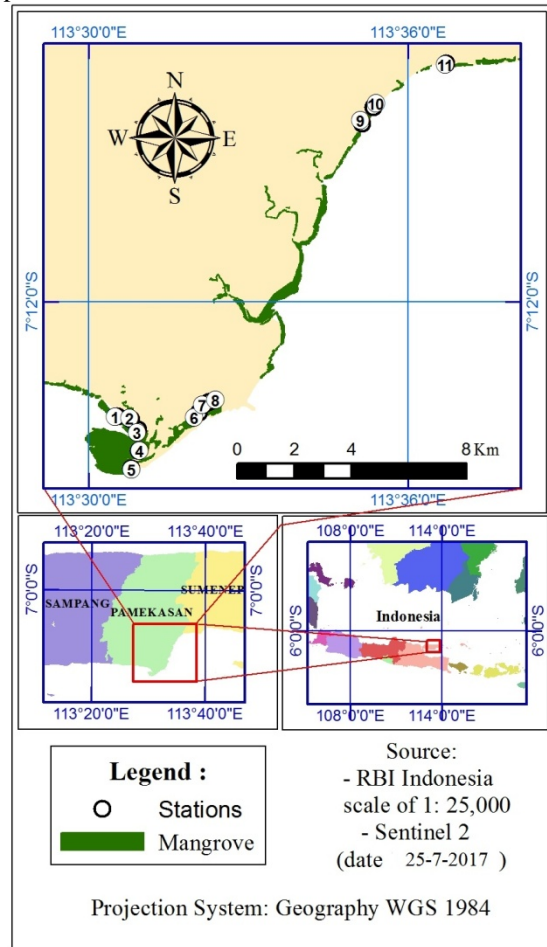
Fig. 1 Map of Research Location

3. RESULTS AND DISCUSSION

Initial stages of the study involved radiometric correction of the Sentinel-2 image. Radiometric correction by converting radian value to at-sensor reflectance. Danoedoro et al. (2015) described this method as proving better and most stable for carbon stock estimation [26], [6].

The results of field measurements on all plots were analyzed, obtained carbon biomass and soil carbon data. Data tested, data test with Kolmogorov-Smirnov normality test [9]. The result of statistical analysis of Kolmogorov-Smirnov normality test obtained values >0.05,

except data result of SAVI vegetation index which had amount 0, shows typically distributed data.

3.1. Modeling Estimation of Total Carbon Mangrove Content (Carbon Biomass and Soil Carbon) with Value of Vegetation Index.

The initial phase of total estimation of mangrove carbon was carried out with non-linear regression of total carbon (carbon biomass and soil carbon) with Sentinel 2 image vegetation index value (24 species of vegetation index). The coefficient of determination (R^2) showed a weakly correlated result if $R^2 < 0.5$ [27], [28], [29], [30], [14], [31]. The result of determination value with regression exponential, logarithmic, polynomial and power/geometry got value $R^2 < 0.5$ (value R^2 biggest 0.064). The value of R^2 shows the regression between total mangrove carbon and vegetation index is not feasible because of the weak correlation value.

3.2. Biomass Carbon Content Estimation Modeling.

The result of determining regression value of exponential, logarithmic, polynomial and power/geometry between a variable of carbon biomass with vegetation index get a value of R^2 was having a good/reliable correlation (value $R^2 > 0.8$). Regression was having values of $R^2 > 0.8$, exponential regression for vegetation index NDVI, NDVI2, NNIP, SVI, MTV2, RDVI, MSR; regression of power/geometry for vegetation index of GNDVI, NDVI, NDVI2, NNIP, SVI, RDVI, MSR (Table 1). SPOT 5 and Landsat TM images obtained the best vegetation index was NDVI with non-linear regression [32], [5]. Worldview-2's best index is DVI, EVI, MRE-SR with allometric equations and 80.9% accuracy [6]. This result differed from this research. The best vegetation index was NNIP (Normalized Near Infrared with power equation/geometry with RMSE value 0.2474 t 100 m^{-2}.

Table 1 RMSE test results and model of the Sentinel 2 image biomass estimation equation

No	Regression of vegetation index	Carbon Biomass Model
1	NNIP power	$y = 280.44519x^{13.63868}$ RMSE = 0.2470 t 100 m^{-2}, $R^2 = 0.8570$
2	NNIP exponential	$y = 0.0000004e^{22.2258646x}$ RMSE = 0.2490 t 100 m^{-2}, $R^2 = 0.8528$
3	GNDVI power	$y = 66.76199x^{6.22939}$ RMSE = 0.2498 t 100 m^{-2},

No	Regression of vegetation index	Carbon Biomass Model
		$R^2 = 0.8038$
4	NDVI power	$y = 20.16317x^{8.33372}$ RMSE = 0.2523 t 100 m^{-2}, $R^2 = 0.8696$
5	NDVI2 power	$y = 20.16317x^{8.33372}$ RMSE = 0.2523 t 100 m^{-2}, $R^2 = 0.8696$
6	SVI power	$y = 20.16317x^{8.33372}$ RMSE = 0.2523 t 100 m^{-2}, $R^2 = 0.8696$
7	MSAVI exponential	$y = 0.00002e^{15.18280x}$ RMSE = 0.2523 t 100 m^{-2}, $R^2 = 0.8692$
8	RDVI power	$Y = 24.08576x^{6.04895}$ RMSE = 0.2523 t 100 m^{-2}, $R^2 = 0.8697$
9	NDVI exponential	$y = 0.00008e^{13.68111x}$ RMSE = 0.2528 t 100 m^{-2}, $R^2 = 0.8689$
10	NDVI2 exponential	$y = 0.00008e^{13.68111x}$ RMSE = 0.2528 t 100 m^{-2}, $R^2 = 0.8689$
11	SVI exponential	$y = 0.00008e^{13.68111x}$ RMSE = 0.2528 t 100 m^{-2}, $R^2 = 0.8689$
12	MSR power	$y = 0.07086x^{4.64446}$ RMSE = 0.2536 t 100 m^{-2}, $R^2 = 0.8687$
13	RDVI exponential	$y = 0.00075e^{12.28222x}$ RMSE = 0.2542 t 100 m^{-2}, $R^2 = 0.8672$
14	MSAVI power	$y = 24.25246x^{9.74722}$ RMSE = 0.2562 t 100 m^{-2}, $R^2 = 0.8696$
15	MSR exponential	$y = 0.00326e^{3.28180x}$ RMSE = 0.2571 t 100 m^{-2}, $R^2 = 0.8595$

Description: X = Vegetation Index Value, n (RMSE) = 80.

ALOS AVNIR-2 image was EVI-2, TVI, ARVI, SAVI, and MSAVI. The MSAVI vegetation index with exponential equations provided the smallest or most accurate standard of error, with above-ground carbon averages of 0.2582-0.5968 t 100 m^{-2} [8]. Kamal (2015) obtained for the best Worldview-2 SAVI vegetation index image with RMSE 1.15, for the best model ALOS AVNIR-2 NDVI vegetation index with RMSE 1.31, for Landsat TM image of the best vegetation index SR with RMSE 1.23 [21]. Muhsoni et al. (2018) obtained an appropriate vegetation index for estimation of estuarine mangrove biomass was the NDVI vegetation index with 0.089 t 100 m^{-2} RMSE [33].

3.3. Soil Carbon Content Estimation Modeling.

Soil carbon modeling with soil carbon calculation equation (Ct = Kd x ρ x% organic C). kd = Depth of soil / sediment (cm), ρ = density of action (g cm^{-3}) and% C organic (% C depth 0-15 cm, 15-50 cm and >50 cm). The equation of the modeling result is:

Y= ((15*x1*x2)+(35*x1*x3)+((x5-50)*x1*x4)

Description: x1=bulk density (g cm^{-3}), x2=% C depth 0-15cm, x3=% C depth 15-50 cm, x4=% C depth >15cm, x5=sediment depth (cm). The RMSE test results for this model was 0.5039 t 100 m^{-2}.

Soil carbon modeling with regression of soil carbon with vegetation index with exponential, logarithmic, polynomial, power/geometric and linear regression got determination value R^2 <0.5 (the most significant R^2 value 0.209). The amount of R^2 found that all regression models between soil carbon and vegetation index are not feasible to use because they have a weak correlation.

Soil carbon modeling with multiple regression using several simulations:

- Regression equation with two variables, namely X1=vegetation index value, and X2=sediment depth.
- Regression equation with 3 variables, namely X1=vegetation index value, X2=sediment depth and X3= bulk density,
- Regression equation with 6 variables, namely X1=vegetation index value, X2=sediment depth, X3=bulk density, X4=% C depth 0-15 cm, X5=% C depth 15-50 cm and X6=% C depth >50 cm.

The result of model got a coefficient value of determination of multiple regression with six variable got value 89.8%-90.7%, showed very good regression. Multiple regression with three variables got the value of determination 52.8% - 58.7%, The value showed good enough regression. Regression of 2 variables got a determination value of 32.8% -37.8%, showed poor regression. Regression of 6 variables, three variables and two variables that had the highest determination value 4 was the vegetation index VIRE, VIRRE, WVVI, and NDRE.

The RMSE test result for the best six variable modeling used NDRE (Normalized difference Red-Edge index) value of RMSE 0.5011 t 100 m^{-2} and WVVI (WorldView Improved Vegetative Index) vegetation index of RMSE 0.5011 t 100 m^{-2} value. Multiple modeling for the three highest RMSE test variables were VIRE vegetation index with RMSE 0.5924 t 100 m^{-2} and VIRRE vegetation index equation with RMSE 0.934 t 100 m^{-2}. Multiple modeling for two

highest variables using NDRE vegetation index equation with RMSE 0.7747 t 100 m^{-2} and WVVI vegetation index equation with RMSE 0.7747 t 100 m^{-2}.

3.4. Determination of Best Model of Total Mangrove Carbon Content

The determination of the total mangrove carbon content model was done by combining the biomass carbon estimation model with the soil estimate model. In this modeling some simulations were performed:

1. Model 1 with equation 1-1:

y = (280.44519*(X1)$^{13.63868}$) + (-3.42587-3.44731*X2 + 0.01795*X3 + 2.81797*X4 + 25.45099*X5 + 17.43371*X6 + 50.02014*X7)

Description: X1=NNIP vegetation index, X2=NDRE vegetation index, NNIP= $\frac{NIR1}{(NIR1+R+G)}$, NDRE= $\frac{NIR1-RE}{NIR1+RE}$, NIR1=band 8, R=band 4, G=band 3, RE=band 5, X3=Depth of sediment (cm), X4=bulk density (g cm^{-3}), X5=% C depth 0-15cm, X6=% C depth 15-50 cm, X7=% C depth >15cm. RMSE=0.47786 t 100 m^{-2}, % RMSE=16.12%, Mean=2.84 t 100 m^{-2}, Std=0.59 t 100 m^{-2}, Min=1.39 t 100 m^{-2}, Max=5.47 t 100 m^{-2}, Total Carbon mangrove=187,398.0 t C, Average C ha^{-1} = 283.61 t C ha^{-1} (Fig. 2).

Equation 1-2:

y = (280.44519*((X1)$^{13.63868}$)) + (-3.42587-3.44731*X2 + 0.01795*X3 + 2.81797*X4 + 25.45099*X5 + 17.43371*X6 + 50.02014*X7)

Description: X1=NNIP vegetation index, X2=WVVI vegetation index, NNIP= $\frac{NIR1}{(NIR1+R+G)}$, WVVI= $\frac{NIR2-RE}{NIR2+RE}$, NIR1=band 8, R=band 4, G=band 3, RE=band 5, X3=Depth of sediment (cm), X4= bulk density (g cm^{-3}), X5=% C depth 0-15cm, X6 =% C depth 15-50 cm, X7=% C depth >15cm. RMSE=0.47786 t 100 m^{-2}, % RMSE=16.12%, Mean=2.86 t 100 m^{-2}, Std=0.68 t 100 m^{-2}, Min=1.28 t 100 m^{-2}, Max=9.11 t 100 m^{-2}, Total Carbon mangrove=187,790.3 t C, Average C ha^{-1} = 284.20 t C ha^{-1} (Fig. 3).

2. Model 2 with the equation:

y = (280.44519*((X1)$^{13.63868}$)) + (3.08347-1.7259*X2 + 0.01640*X3 + 1.52865*X4)

Description: X1 = NNIP vegetation index, X2 = VIRRE vegetation index, NNIP = $\frac{NIR1}{(NIR1+R+G)}$, VIRRE = $\frac{NIR1}{RE}$, NIR1=band 8, R=band 4, G=band 3, RE=band 5, X3=Sediment depth (cm), X4= bulk density (g cm^{-3}). RMSE=0.56398 t 100 m^{-2}, % RMSE=19.03%, Mean=2.95 t 100 m^{-2}, Std=0.69 t 100 m^{-2}, Min=1.10 t 100 m^{-2}, Max=5.48 t 100 m^{-2},

total Carbon mangrove=194,301.0 t C, Average C ha^{-1} = 294.05 t C ha^{-1} (Fig. 4).

3. Model 3 with the equation:

y = (280.44519*((X1)$^{13.63868}$)) + (3.34631-7.78604*X2 + 0.02042*X3)

Description: X1=NNIP vegetation index, X2=NDRE vegetation index, NNIP= $\frac{NIR1}{(NIR1+R+G)}$, NDRE= $\frac{NIR1-RE}{NIR1+RE}$, NIR1=band 8, R=band 4, G=band 3, RE=band 5, X3=Depth of sediment (cm). RMSE=0.7295 t 100 m^{-2}, % RMSE=24.63%, Mean=3.29 t 100 m^{-2}, Std=0.73 t 100 m^{-2}, Min=1.23 t 100 m^{-2}, Max=6.38 t 100 m^{-2}, Total Carbon mangrove=216,574.4 t C, Average C ha^{-1} =327.76 t C ha^{-1} (Fig. 5)

4. Model 4 with the equation:

y = (280.44519*((X1)$^{13.63868}$)) + (3.08347-1.7259*X2 + 0.01640*X3 + 1.52865*X4)

Description: X1=NNIP vegetation index, X2=VIRRE vegetation index, NNIP $= \frac{NIR1}{(NIR1+R+G)}$, VIRRE $= \frac{NIR1}{RE}$, NIR1=band 8, R=band 4, G=band 3, RE=band 5, X3=average sediment depth (100.63 cm), X4=average density of action (1.02 g cm^{-3}). RMSE=1.0043 t 100 m^{-2}, % RMSE=33.89%, Mean=3.2 t 100 m^{-2}, Std=0.44 t 100 m^{-2}, Min=1.073 t 100 m^{-2}, Max=5.05 t 100 m^{-2}, Total Carbon mangrove=210,619.7 t C, Average C ha^{-1} =318.75 t C ha^{-1} (Fig. 6).

The ALOS AVNIR-2 image obtained the best vegetation index for above ground carbon was EVI1 with error 22.9% and for underground carbon index of GEMI vegetation with 40% error [26]. These results were different from those produced in this study. Compared to this research, this study obtained better accuracy with an error of 16.2%.

4. CONCLUSION

The best modeling of Sentinel-2 for estimation of mangrove carbon is model 1. Model 1 with the merging of NNIP vegetation index equation using the power/geometric regression for biomass carbon estimation and six variable regression (NDRE or WVVI vegetation index, sediment depth, soil density, % C depth 0-15 cm, % C depth of 15-50 cm and % C depth >50 cm). RMSE test resulted in 0.4778 t 100 m^{-2} and RMSE % of 16.12%. Model 2 estimates of biomass using NNIP vegetation index and soil carbon estimate using multiple regression of 3 variables (VIRRE vegetation index, sediment depth, soil density). RMSE test result was 0.5639 t 100 m^{-2} and RMSE 19.03 %. Model 3 biomass estimation using NNIP vegetation index and soil estimate using two variables (NDRE vegetation index and sediment depth). RMSE test result was 0.7295 t 100 m^{-2} and RMSE 24.63%. The four merger model between the NNIP vegetation index equations uses the power/geometric regression for biomass carbon estimation and the three variable multiple regression (VIRRE vegetation index, average sediment depth value 100.63 cm, 1.02 g cm^{-3} soil density). RMSE test result is 1.0043 t 100 m^{-2} and % RMSE 33.89%.
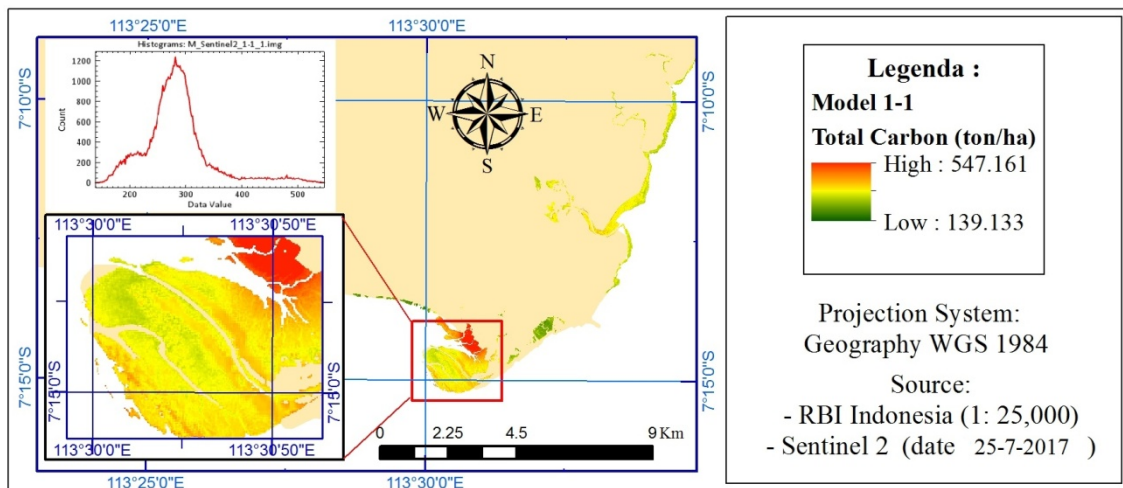
Fig. 2 Map of mangrove carbon and histogram table results Model 1-1.
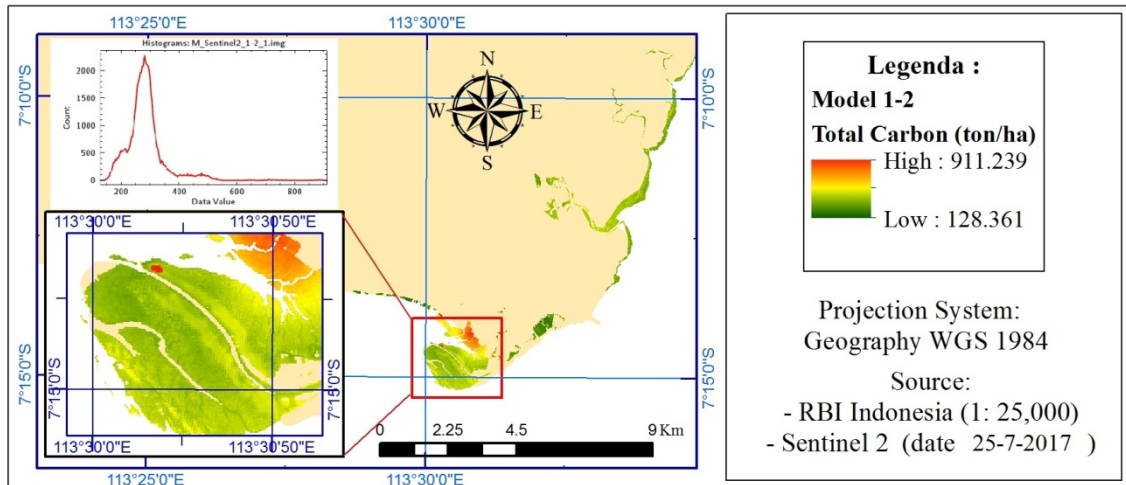
Fig. 3 Map of mangrove carbon and histogram table results Model 1-2.
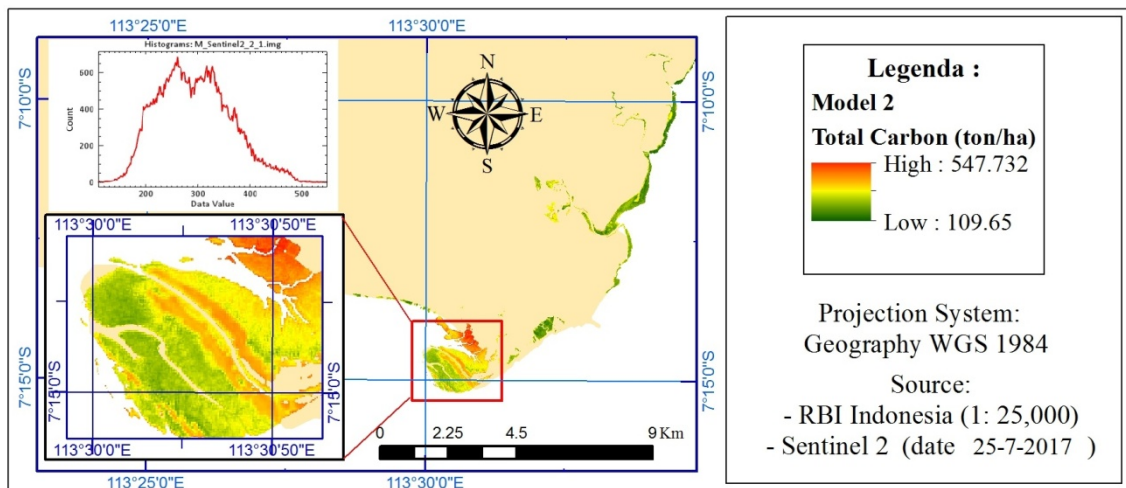
Fig. 4 Map of mangrove carbon and histogram table results Model 2.
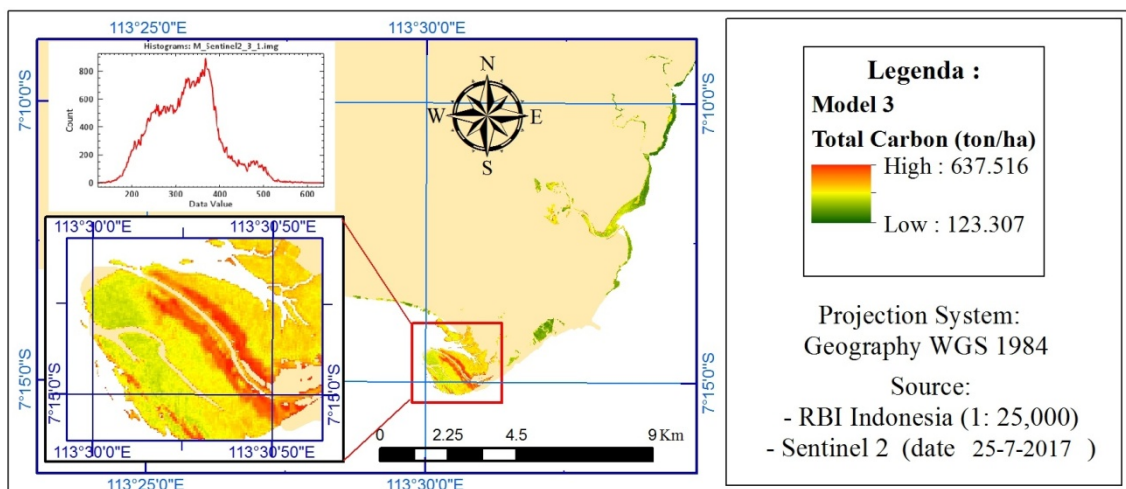
Fig. 5 Map of mangrove carbon and histogram table result of Model 3.
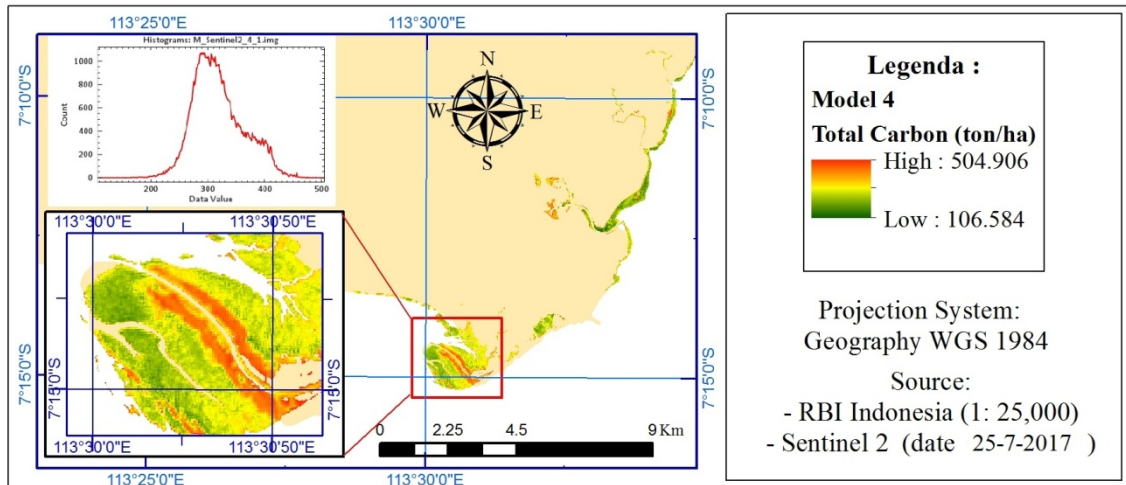
Fig. 6 Map of the mangrove carbon and histogram table result of Model 4.

5. ACKNOWLEDGMENTS

6. REFERENCES

[1] Jennerjahn T. C. and Ittekkot V., Relevance of mangroves for the production and deposition of organic matter along tropical continental margins. *Naturwissenschaften*, vol. 89, no. 1, 2002, pp. 23–30.

[2] Heumann B. W., Satellite remote sensing of mangrove forests: Recent advances and future opportunities. *Prog. Phys. Geogr.*, vol. 35, no. 1, 2011, pp. 87–108.

[3] Hirata Y., Tabuchi R., Patanaponpaiboon P., Poungparn S., Yoneda R., and Fujioka Y., Estimation of aboveground biomass in mangrove forests using high-resolution satellite data. *J. For. Res.*, vol. 19, no. 1, 2014, pp. 34–41.

[4] Ishii T. and Tateda Y., Leaf area index and biomass estimation for mangrove plantation in Thailand, *IGARSS 2004. 2004 IEEE Int. Geosci. Remote Sens. Symp.*, vol. 4, no. c, 2004, pp. 2323–2326.

[5] Li X., Gar-On Yeh A., Wang S., Liu K., Qian J. and Chen X., Regression and analytical models for estimating mangrove wetland biomass in South China using Radarsat images. *Int. J. Remote Sens.*, vol. 28, no. 24, 2007, pp. 5567–5582.

[6] Candra E. D., Hartono, and Wicaksono P., Above Ground Carbon Stock Estimates of Mangrove Forest Using Worldview-2 Imagery in Teluk Benoa, Bali. *IOP Conf. Ser. Earth Environ. Sci.*, vol. 47, no. 1, 2016, pp. 1-11.

[7] Drusch M., Del Bello, U., Carlier S., Colin O., Fernandez V., Gascon F., Hoersch B., Isola C., Laberinti P., Martimort P., Meygret A., Spoto F., Sy O., Marchese F., Bargellini P., "Sentinel-2: ESA's Optical High-Resolution Mission for GMES Operational Services. *Remote Sens. Environ.*, vol. 120, 2012, pp. 25–36.

[8] Danoedoro P., Kristian G., and Rahmi K. N. I., Influence of Radiometric Correction Method of ALOS AVNIR-2 Image Against Accuracy of Estimation of Trunk Vegetation Estimation in City of East Semarang. *Research Gate*. 2015. pp. 1-16.

[9] Lillesand T. M., and Kiefer R. W., Remote sensing and image interpretation, 2003 pp. 1–2.

[10] Otsu N., A Threshold Selection Method from Gray-Level Histograms, *IEEE Trans. Syst. Man. Cybern.*, vol. 9, no. 1, 1979, pp. 62–66.

[11] El-Shirbeny M. A., Abdellatif B., Ali A.-E. M., and Saleh N. H., Evaluation of Hargreaves based on remote sensing method to estimate potential crop evapotranspiration, *Int. J. GEOMATE*, vol. 11, no. 23, 2016, pp. 2143–2149.

[12] Davidson R. and Mackinnon J. G., *Econometric Theory and Method*. Oxford University Press, USA, 1999.

[13] Gumbricht T., Hybrid Mapping of Pantropical Wetlands from Optical Satellite Images, Hydrology, and Geomorphology, in *Remote sensing of wetlands*, R. W. Tiner, M. W. Lang, and V. V. Klemas, Eds. Boca Raton: CRC Press is an imprint of Taylor & Francis Group, an Informa business, 2015, pp. 435–454.

[14] Clark M. L., Roberts D. A., Ewel J. J., and

Clark D. B., Estimation of tropical rainforest aboveground biomass with small-footprint lidar and hyperspectral sensors, *Remote Sens. Environ.*, vol. 115, no. 11, 2011, pp. 2931–2942.

[15] Kulawardhana R. W., Popescu S. C., and Feagin R. A., Fusion of lidar and multispectral data to quantify salt marsh carbon stocks, *Remote Sens. Environ.*, vol. 154, 2014, pp. 345–357.

[16] Cartus O., Kellndorfer J., Walker W., Franco C., Bishop J., Santos L., and Fuentes J. M.M., A national, detailed map of forest aboveground carbon stocks in Mexico," *Remote Sens.*, vol. 6, no. 6, 2014, pp. 5559–5588.

[17] Hu T., Su Y., Xue B., Liu J., Zhao X., Fang J., and Guo Q., Mapping Global Forest Aboveground Biomass with Spaceborne LiDAR, Optical Imagery, and Forest Inventory Data," *Remote Sens.*, vol. 8, no. 7, 2016, p. 565.

[18] Alan J., Castillo A., Apan A. A., Narayan T., and Iii S. G. S., Geoderma Soil C quantities of mangrove forests , their competing land uses , and their spatial distribution in the coast of Honda Bay , Philippines. *Geoderma*, vol. 293, 2017, pp. 82–90.

[19] Köhl M., Magnussen S., and Marchetti M., *Sampling Methods, Remote Sensing and GIS Multiresource Forest Inventory*, vol. 3, no. 2–3. 2006, pp. 91-156.

[20] Weng Q., *Remote Sensing and GIS Integration Theories, Methods, and Applications*. New York Chicago San Francisco Lisbon London Madrid Mexico City Milan New Delhi San Juan Seoul Singapore Sydney Toronto: Mc Graw Hill, 2010, pp. 169-182.

[21] Kamal M., Remote Sensing for Multi-scale Mangrove Mapping," *Sch. Geogr.*, 2015, pp. 81-106.

[22] Thenkabail P. S., *Remotely Sensed Data Characterization, Classification, and Accuracies*. Boca Raton: Taylor & Francis Group, LLC, 2016, pp. 219-229.

[23] Chuvieco E., Li J., and Yang X., *Advances in Earth Observation of Global Change*. New York: Springer, 2010, pp 69-78.

[24] Alparone L., Aiazzi B., Baronti S., and Garzelli A., *Remote Sensing Image Fusion*. 2015, pp. 151-170.

[25] Vicharnakorn P., Shrestha R. P., Nagai M., Salam A. P., and Kiratiprayoon S., Carbon stock assessment using remote sensing and forest inventory data in Savannakhet, Lao PDR, *Remote Sens.*, vol. 6, no. 6, 2014, pp. 5452–5479.

[26] Wicaksono P., Danoedoro P., Hartono, and Nehren U., Mangrove biomass carbon stock mapping of the Karimunjawa Islands using multispectral remote sensing, *Int. J. Remote Sens.*, vol. 37, no. 1, 2016, pp. 26–52.

[27] Thenkabail P. S., *Land Resources Monitoring , Modeling , and Mapping With Remote Sensing*, vol. II. Boca Raton: CRC Press is an imprint of Taylor & Francis Group, 2016, pp. 3-22.

[28] Fatoyinbo T., *Remote Sensing of Biomass - Principles and Applications*, no. 15. 2012, pp. 77-98

[29] Zhang W., *Ecological Modelling*. New York: Nova Science Publishers, Inc, 2012, pp. 15-40

[30] Rock B. N., Vogelmann J. E., Williams D. L., Vogelmann A. F., and Hoshizaki T., Remote detection of forest damage, *Bioscience*, vol. 36, no. 7, 1986, pp. 439–445.

[31] Zheng G., Chen J. M., Tian Q. J., Ju W. M., and Xia X. Q., Combining remote sensing imagery and forest age inventory for biomass mapping, *J. Environ. Manage.*, vol. 85, no. 3, 2007, pp. 616–623.

[32] Hamdan O., Khairunnisa M., Ammar A., Mohd Hasmadi I., and Khali Aziz H., Mangrove Carbon Stock Assessment By Optical Satellite Imagery, *J. Trop. For. Sci.*, vol. 25, no. 4, 2013, pp. 554–565.

[33] Muhsoni F. F., Sambah A. B., Mahmudi M., and Wiadnya D. G. R., Comparison of Different Vegetation Indices for Assessing Mangrove Density Using Sentinel-2 Imagery, *Int. J. GEOMATE*, vol. 14, no. 45, 2018, pp. 42–51.